

Turbulent boundary layer manipulation by longitudinal embedded vortices

by

G. M. Di Cicca, M. Onorato, G. Iuso

Department of Aerospace Engineering, Politecnico di Torino
C.so Duca degli Abruzzi, 24 - I 10129 Torino, ITALY

and

P. G. Spazzini

Centro Studi Dinamica dei Fluidi – CNR
C.so Duca degli Abruzzi, 24 - I 10129 Torino, ITALY

ABSTRACT

Digital Particle Image Velocimetry has been applied to the study of a flat plate turbulent boundary layer "manipulated" by streamwise large scale vortices. The vortical field was generated by a series of jets at 45 degrees with respect to the wall and in a plane transversal to the mean flow direction. Images in planes perpendicular and parallel to the wall were analyzed.

Results from the manipulated flow are compared to the ones from the natural boundary layer. Measurements in planes at $y \approx 20$ reveal that, at least for the flow condition tested here, there is no evidence of changes in the global organization of structures in the near wall flow.

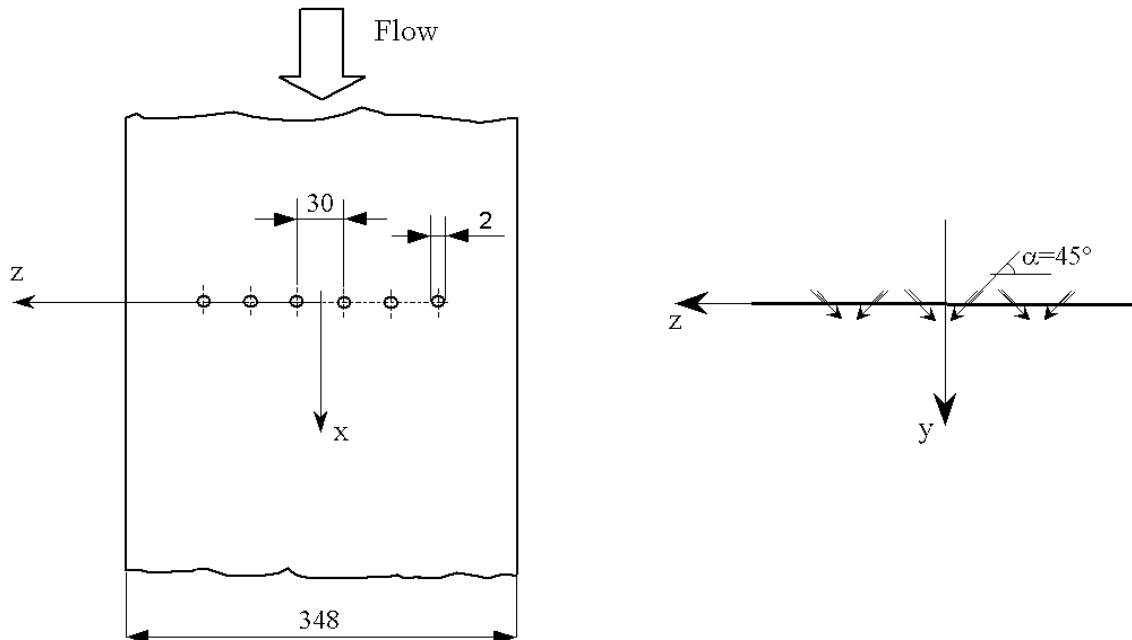


Fig. 1. Sketch of the flat plate with jet holes configuration and reference system. Dimensions in millimeters.

1. INTRODUCTION

The development of the flow field produced by vortex generator jets (VGJ) has been the subject of many studies (Pauley and Eaton, 1998, Hasegawa et al., 1998, Shelby et al., 1992, Johnston and Nishi, 1990), whose aim was the control of flow separation in adverse pressure gradients. Recently Schoppa and Hussain (1998), using DNS data of turbulent channel flows, demonstrated that spanwise integrated skin friction reduction may be obtained by a spanwise row of counter rotating large scale streamwise vortices centered at the channel center-line. With reference to these new developments, the present investigation deals with the characteristics of the flow in the buffer layer and the inner part of the logarithmic region of a turbulent boundary layer, in presence of streamwise embedded large scale vortices produced by VGJ.

2. EXPERIMENTAL TECHNIQUE

The experiment was carried out in the Hydra water tunnel of CNR-CSDF. This facility is a closed loop, open flow channel with $350 \times 500 \times 1800 \text{ mm}^3$ test section. Measurements were taken over a flat plate 2050 mm long, spanning the whole test section, with imposed transition at the leading edge. An array of longitudinal vortices is generated by water jets, injected in the transversal plane at $x=0$ (at 1400 mm from the leading edge) through 6 holes (2 mm diameter), drilled at pitch angles of alternatively 45 and -45 degrees, through the plate along its span (Fig.1). The jets configuration produces three couples of counter-rotating vortices. The distance between two adjacent holes is 30 mm, corresponding to about 500 viscous lengths at the natural test condition. The ratio between the mass flow rate of the 6 jets and the mass flow rate of the boundary layer is 0.003.

The flow is seeded with spherical solid particles, 2 microns nominal diameter. A double-pulsed light sheet is provided by a Nd-YAG laser source (200 mJ and 8 ns per pulse). Images are captured by a digital video camera Kodak MEGAPLUS ES1.0 (1008×1012 pixels) and analyzed via cross-correlation technique. Results obtained by lighting the planes (y,z), (x,y) and (x,z) will be shown in this paper.

In the (y,z) planes the interrogation window is 16×16 pixels which corresponds to a physical dimension of $1.2 \times 1.2 \text{ mm}^2$, at $x = 250 \text{ mm}$. An interrogation spot size of 32×32 pixels and a 50% window overlap are used for the (x,y) plane, corresponding to $0.3 \times 0.3 \text{ mm}^2$ and for the (x,z) plane, corresponding to $1.2 \times 1.2 \text{ mm}^2$.

The natural boundary layer at the injection section is characterized by $Re_q = 1160$ and $u_t/U_e = 0.052$.

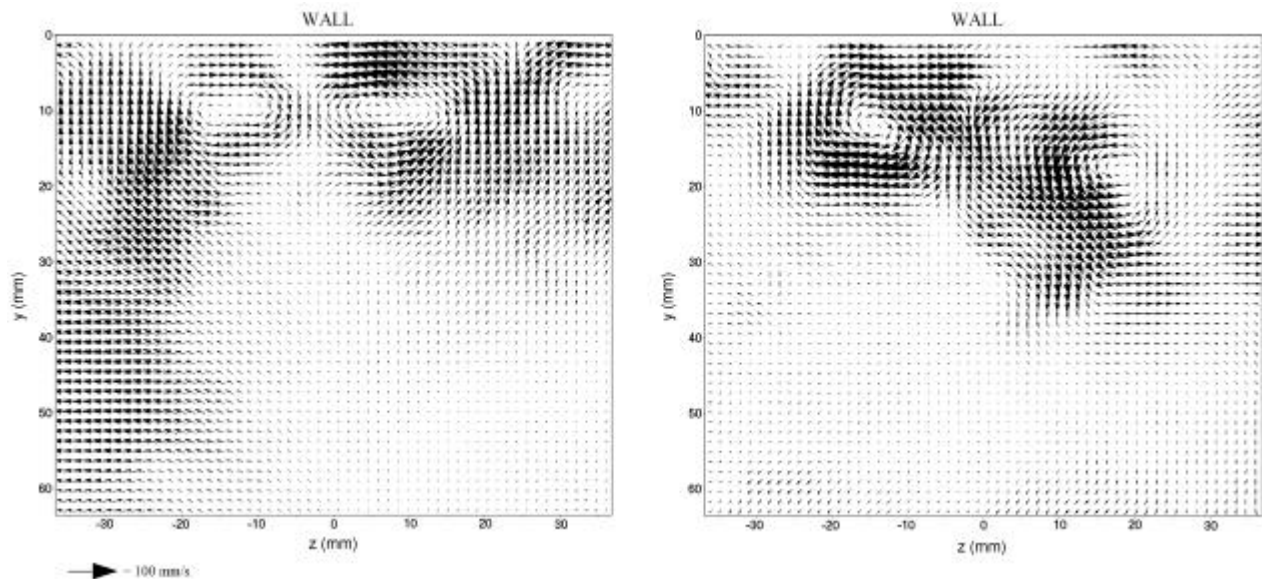


Fig. 2. Instantaneous vectorial velocity fields in the (y,z) plane at $x=130\text{mm}$.

3. RESULTS

In Figs. 2a and 2b rear end views, at two different instants, of the velocity flow field in the plane (y,z) at $x = 130$ mm are shown. It is evident the unsteady nature of the vortical configuration produced by VGJ. In Figs. 3a and 3b mean values, obtained by averaging 100 couples of PIV images, respectively at $x = 130$ mm and $x = 250$ mm, are reported. The two counter rotating vortices in the central part of the flat plate, approximately symmetric with respect to the $z = 0$ plane, are visible. The vortices appear to be completely immersed in the boundary layer, whose thickness for the natural flow is about 43 mm at $x = 250$ mm. Close to the wall, a region of colliding spanwise jets is evident for $-15 \text{ mm} \leq z \leq 15 \text{ mm}$. In the proximity of $z = 0$ mm, farther from the wall, an up flow region is present, in contrast with a down flow region located around $z = \pm 30$ mm.

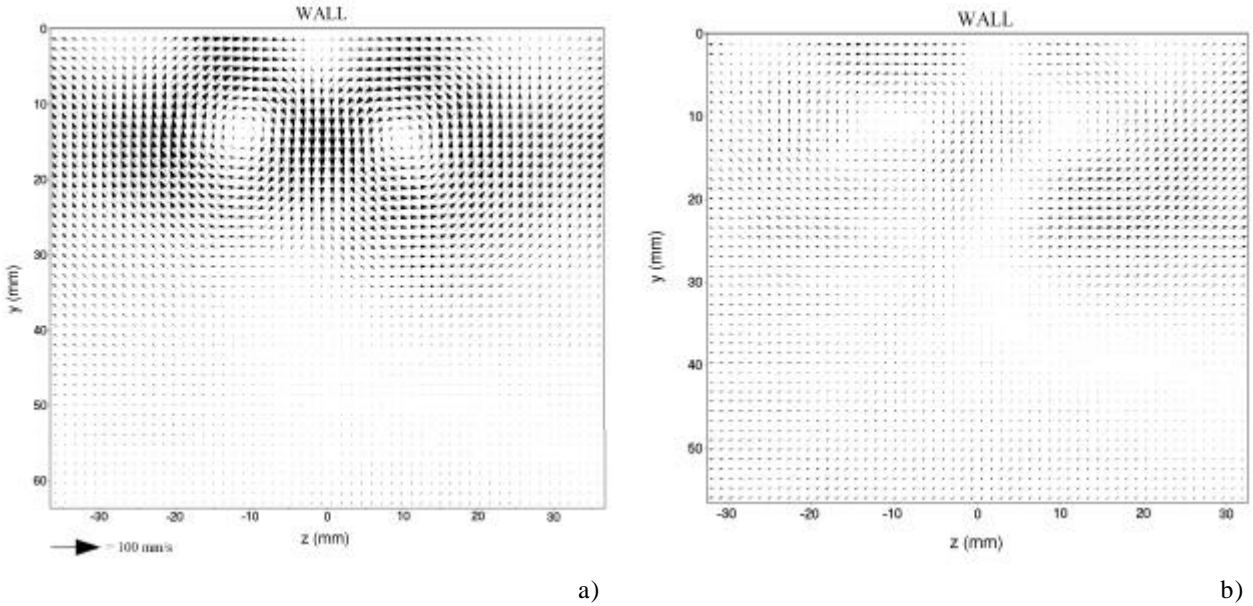


Fig. 3. Mean vectorial velocity flow fields in the (y,z) plane at $x=130$ mm (a) and $x=250$ mm (b).

In table 1 the maximum wall normal and spanwise mean velocities are reported. As it can be observed, disturbance velocities are quite small; in particular, in the plane $x = 250$ mm, they are within 5% of the external velocity.

x(mm)	Max inflow velocity (V/U_e)	Max outflow velocity (V/U_e)	Max spanwise velocity (W/U_e)
130	0.096	-0.056	0.076
250	0.030	-0.019	0.047

Tab. 1. Maximum disturbance velocities.

Mean velocity profiles were measured for the natural and the manipulated boundary layers, in the up flow ($z = 0$ mm) and down flow ($z \approx 30$ mm) regions and in correspondence of the vortex axis ($z \approx 11$ mm), at $x = 250$ mm, in the plane (x,y) . Values were obtained by averaging 1000 couples of images. In Figs. 4a and 4b the longitudinal and wall normal mean velocity profiles are displayed in the lower part of the boundary layer ($y^+ \leq 150$). The U velocity profiles, Fig. 4a, correspond closely to velocity profiles as measured by Johnston and Nishi (1990) in a similarly manipulated flow. Fluid inflow ($z \approx 30$ mm) increases the mean momentum in the inner region of the boundary layer, which supposedly raises the local skin friction value, t_w , with respect to the natural boundary layer case. Outflow in the central part of the vortex couple ($z = 0$ mm), on the other side, exhibits a reduction in the mean momentum, supposedly lowering the local value of t_w . At $z = 11$ mm, the velocity profile still shows a behavior similar to the one

of the outflow region, although with reduced intensity. With reference to the colliding spanwise jets region, it may be deduced that in this region and for the present flow condition the manipulation results in a lower skin friction value. The amount of inflow and outflow velocities as a function of the distance from the wall is shown in Fig. 4b, where it is shown that maximum wall normal velocities are always lower than 3% of the external velocity.

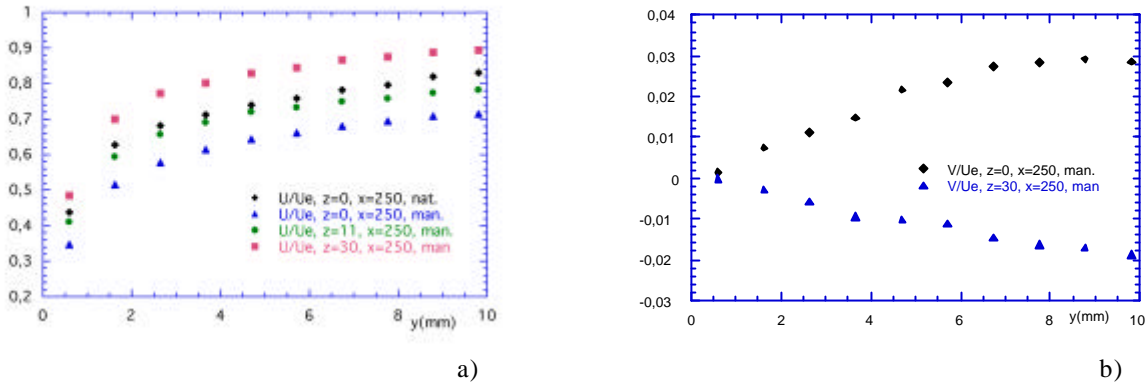


Fig. 4. Mean longitudinal (a) and wall normal (b) velocity profiles, at $x=250\text{mm}$.

The spanwise distribution of the mean transverse component of velocity W is shown in Fig. 5a at a distance from the wall of 20 viscous units ($y^+ = 20$) and at about 250 mm from the injection section. Maximum and minimum values in this distribution confirm the weakness of the imposed vortical field. In Fig. 5b the percent variation of the manipulated mean longitudinal velocity with respect to the natural boundary layer mean velocity shows a reduction in the central part between the two counter rotating vortex axis and an increase of velocity in the external part.

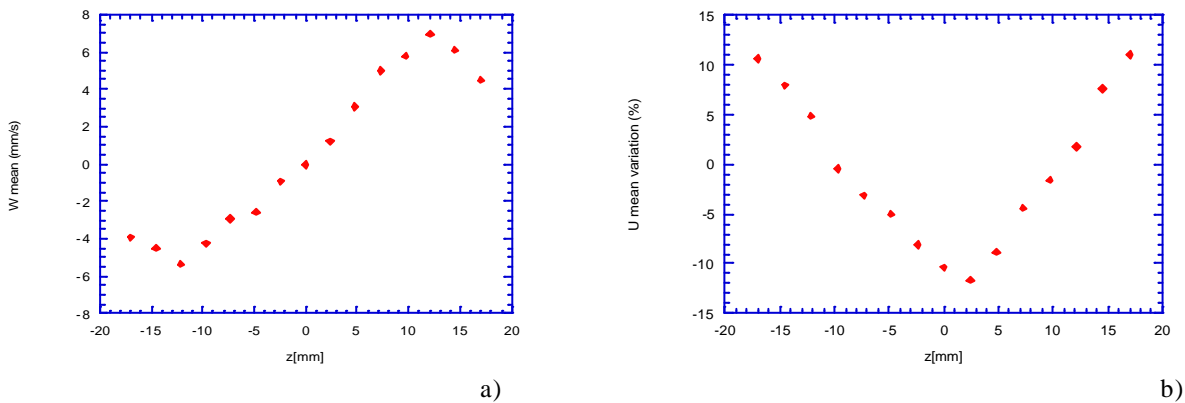


Fig. 5. Mean spanwise velocity W -distribution (a) and percent variation of mean longitudinal velocity U -distribution (b) at $x=250\text{mm}$ and $y^+ > 20$.

To explain the modifications of the boundary layer mean velocity profiles caused by the experimented manipulation, a first thinking is toward the transport of mean momentum in the direction of the wall for the inflow section and away from the wall for the outflow section. This is consistent with the observed results, at least on a qualitative basis. Moreover a direct action of the flow manipulation on turbulence regeneration mechanisms cannot be excluded.

In order to observe if the colliding spanwise jets and the wall inflow and outflow momentum influence the streaky structured wall velocity field, the double spatial correlation function of the velocity components in the plane parallel to the wall has been computed. Figs. 6a and 6b report the double spatial correlation functions of the longitudinal velocity fluctuation, R_{uu} , respectively for the natural and manipulated flow. Correlograms show an elliptical shape of peaks, which presents a width of about 100 wall units for both cases. Analogous results have been found by Carlier et al. (1999).

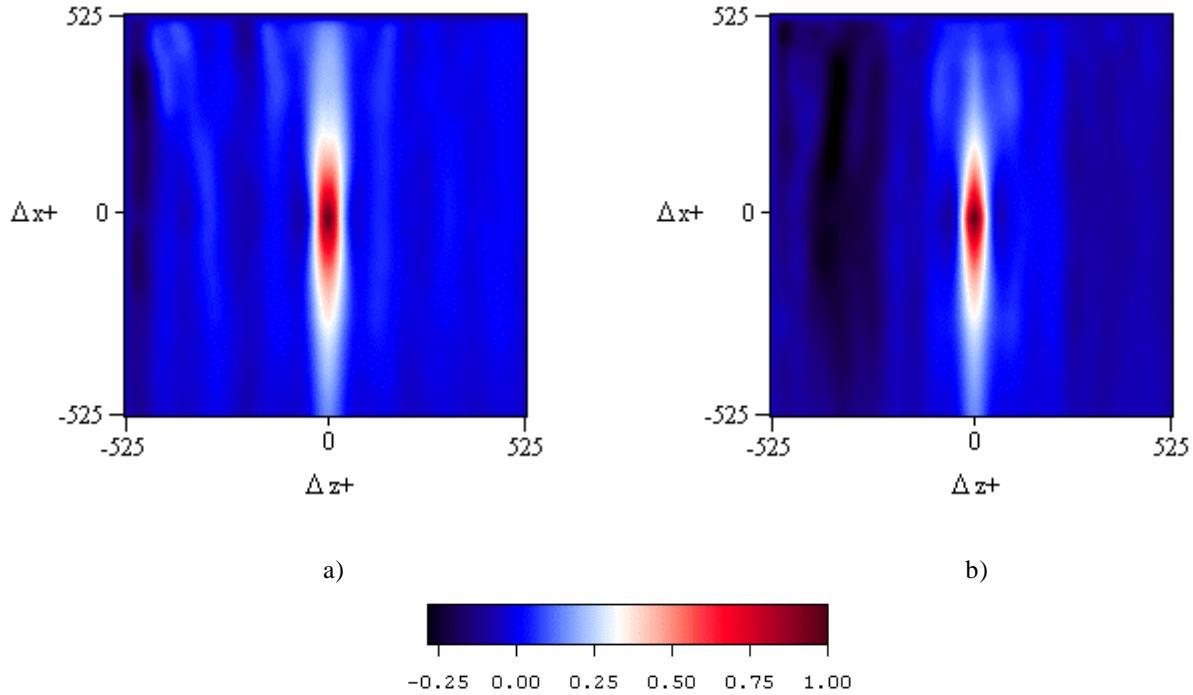


Fig. 6. Double spatial correlation R_{uu} , at $y^+ \gg 20$, in the natural case (a) and manipulated case (b).

From the comparison between the two cases no strong differences are evident so that the global organization of the structures in the near wall flow appears to be similar, at least for this low level of manipulation.

4. CONCLUSIONS

Particle Image Velocimetry has been applied for studying the turbulent boundary layer flow manipulated by embedded streamwise large scale vortices. Fields in planes normal and parallel to the wall have been described in order to characterize the manipulated flow. Comparisons with the natural boundary layer showed a reduction in the mean momentum in the central part of the vortex couple (outflow region). An opposite behaviour is present in the region around $z \approx 30$ mm.

Double spatial correlations of the velocity components in the plane (x,z) have been computed. No evidence of modifications in the global flow organization has been noticed, at least for this low level of manipulation.

Further investigations are required in order to optimize the several parameters involved in the problem, such as the ratio between jet mass flow rate and boundary layer mass flow rate, jet orientation or jet location.

REFERENCES

Carlier J., Foucault J. M., Dupont P., and Stanislas M. Experimental study of near wall turbulence using Particle Image Velocimetry, *Proceedings of the 3th International Workshop on Particle Image Velocimetry*, Santa Barbara, CA., USA, 1999.

Di Cicca G. M., Onorato M., Iuso G., Bollito A. and Spazzini P. G. Experimental study of near wall turbulence using Particle Image Velocimetry, *Proceedings of the 3th International Workshop on Particle Image Velocimetry*, Santa Barbara, CA., USA, 1999.

Hasegawa H., Matsuuchi K., and Yamakami J. The mechanism of active boundary layer control using vortex generator jets. *Proceedings of the 21st ICAS Congress*, Melbourne, Australia, A98-31545 ICAS Paper 98-3.4.3, 1998.

Johnston J. P. and Nishi M. Vortex generator jets - means for flow separation control. *AIAA Journal*, Vol. 28, No. 6, pp 989-994, 1990.

Pauley W. R. and Eaton J. K. Experimental study of the development of longitudinal vortex pairs embedded in a turbulent boundary layer. *AIAA Journal*, Vol. 26, No. 7, pp 816-823, 1998.

Shelby G. V., Lin J. C., and Howard F. G. Control of low-speed turbulent separated flow using jet vortex generators. *Experiments in Fluids*, Vol. 12, pp 394-400, 1992.